First-principles Green-Kubo method for thermal conductivity calculations

Jun Kang and Lin-Wang Wang

A First-Principles Green-Kubo Method for Thermal Conductivity Calculation

Jun Kang and Lin-Wang Wang[*]

Materials Sciences Division, Lawrence Berkeley National Laboratory, Berkeley, California 94720, United States

We present a first-principles approach to calculate the phonon thermal conductivity based on the Green-Kubo formalism. In this approach, the density functional theory energy is distributed to each atom, and a two-step method in the molecular dynamics is introduced to avoid the atomic position $\mathbf{R}$ wrapping problem in a periodic system when the heat current is calculated. We show that this first-principles Green-Kubo approach is particularly suitable for disordered systems like amorphous and liquid, where the thermal conductivities are small due to strong phonon scattering but difficult to be calculated using anharmonic interaction energy. We have applied our method to liquid Ar, liquid Si and amorphous Si. The calculated thermal conductivities agree well with previous theoretical and experimental results. We have also compared our new method to previous works combining first-principles simulations with the Green-Kubo formalism.

Thermal conductivity is an important fundamental property of materials. For semiconductors, lattice thermal conductivity dominates, and it can be theoretically predicted by various methods. One is to calculate the phonon spectrum and anharmonic interactions, followed by Boltzmann equation[1,2]. However, this approach is not suitable for disorder systems like amorphous and liquid, where the anharmonicity can be rather complex[2], and higher order anharmonicity become important for high temperature. One can also simulate the heat flux directly using non-equilibrium molecular dynamics (MD) with a sustained temperature gradient[3,4]. However, a rather large supercell is needed to get a reasonably small temperature gradient. Another widely used approach is the equilibrium MD based Green-Kubo (G-K) method[5–7], which relates the thermal conductivity with the heat current auto-correlation function (HC-ACF) through the dissipation-fluctuation theorem. It has the advantages of weak system-size dependence and full anharmonicity,[8] and can be applied to both crystal and disordered systems with arbitrary temperatures.

Up to date, the G-K method has mostly been applied with force field (FF) Hamiltonian, where the anharmonicity interaction might not be accurate, and in many cases no adequate FF exists. It is thus much more desirable to use first-principles quantum mechanical methods like the density functional theory (DFT) for the G-K simulations. However, there are two challenges for applying the G-K method in DFT: (1) the heat current is not uniquely defined; (2) there is a technical difficulty to define the position vector $\mathbf{r}$ in a periodic system. Recently, Marcolongo *et al.*[9] showed that the nonuniqueness of the heat current should not affect the final thermal conductivity calculated via the G-K formula. They also used a technique to convert the non-uniquely defined $\mathbf{r}$ operator for a periodic system into ∇ using $[H, \mathbf{r}] = \nabla$. However, their approach requires the solution of a set of linear equations[10] at every MD step, which could be computationally expensive. Besides, there could be nondiffusive heat current term, which makes the HC-ACF decays extremely slow or even diverges[9]. In another work by Carbogno *et al.*[11], a quantum mechanical definition of a stress tensor for a given ion is introduced, in analogous

with the FF counterpart. However, they have ignored the convective term in the heat current[12], which can be important for liquid. Besides, the stress tensor expression is most suitable for all-electron Hamiltonian, not for pseudopotential methods.

In this work, we show a new way to perform first-principles G-K (FP-GK) simulations. We use a partition scheme to assign the DFT energy into each atom, and propose a two-step technique to solve the ill-definition problem of $\mathbf{r}$. The method is tested for Ar liquid, Si amorphous and Si liquid.

In the Green-Kubo method, the lattice thermal conductivity κ_α along a particular direction α is given by[7] (in the current work, we are mostly interested in isotropic disordered system, hence only the diagonal thermal conductivities will be calculated below):

$$\kappa_\alpha = \frac{1}{k_\mathrm{B} T^2 V} \int_0^\infty \langle J_\alpha(t) J_\alpha(0) \rangle dt, \qquad (1)$$

where t is the time, V and T are the system volume and temperature, and J_α is the α component of the lattice heat current vector $\mathbf{J}$. $\langle J_\alpha(t) J_\alpha(0) \rangle$ is the ensemble averaged HC-ACF. $\mathbf{J}$ can be defined as[7,13]:

$$\mathbf{J}(t) = \frac{d}{dt} \sum_i \mathbf{R}_i E_i = \sum_i E_i \mathbf{v}_i + \sum_i \mathbf{R}_i \frac{dE_i}{dt} \qquad (2)$$

where $\mathbf{R}_i$, $\mathbf{v}_i$, and E_i are the position vector, velocity, and the energy (both potential and kinetic) of atom i. The first term in the right side of Eq. 2 corresponds to the diffusion of atoms, thus is the convection term. The second term is a correlation term describing the energy transfer between neighboring atoms. In a FF molecular dynamic (FF-MD) calculation, especially for FF based on pair potential $U(\mathbf{R}_i - \mathbf{R}_j)$, the nonuniqueness of $\mathbf{R}_i$ in the second term of Eq. 2 for a periodic system is resolved by using[13,14]

$$\sum_i \mathbf{R}_i \frac{dE_i}{dt} = \frac{1}{2} \sum_{i \neq j} (\mathbf{F}_{ij} \cdot \mathbf{v}_i) \mathbf{R}_{ij}. \qquad (3)$$

Here $\mathbf{R}_{ij} = \mathbf{R}_i - \mathbf{R}_j$ and $\mathbf{F}_{ij}$ is the atomic pair force calculated by $-dU(\mathbf{R}_{ij})/d\mathbf{R}_{ij}$.

In a DFT G-K calculation, we first need to obtain the atomic potential energy for each atom i. Here we adopt the energy density $\varepsilon(\mathbf{r})$ introduced by Martin $et\ al.$[15]:

$$\varepsilon(\mathbf{r}) = t_0(\mathbf{r}) + e_{\mathrm{xc}}(\mathbf{r}) + e_{\mathrm{CC}}(\mathbf{r}) + e^{\mathrm{NL}}(\mathbf{r}), \qquad (4)$$

with

$$t_0(\mathbf{r}) = \frac{1}{2}\sum_{n\mathbf{k}} f_{n\mathbf{k}}|\nabla\psi_{n\mathbf{k}}(\mathbf{r})|^2,$$

$$e_{\mathrm{xc}}(\mathbf{r}) = \epsilon_{\mathrm{xc}}[\rho^{\mathrm{e}}(\mathbf{r})]\rho^{\mathrm{e}}(\mathbf{r}),$$

$$e_{\mathrm{CC}}(\mathbf{r}) = \frac{1}{8\pi}|\nabla[V_{\mathrm{H}}(\mathbf{r}) + \sum_i V_i^{\mathrm{L}}(\mathbf{r})]|^2,$$

$$e^{\mathrm{NL}}(\mathbf{r}) = \sum_i E_i^{\mathrm{NL}}\delta(\mathbf{r} - \mathbf{R}_i),$$

$$E_i^{\mathrm{NL}} = \sum_{n\mathbf{k}\ell} f_{n\mathbf{k}}\int d\mathbf{r}\psi_{n\mathbf{k}}^*(\mathbf{r})V_{i\ell}^{\mathrm{NL}}(\mathbf{r})\hat{P}_\ell\psi_{n\mathbf{k}}(\mathbf{r}).$$

Here $\psi_{n\mathbf{k}}$, and $f_{n\mathbf{k}}$ are the wavefunction and occupation number for the nth band with wave vector $\mathbf{k}$. ϵ_{xc} is the exchange-correlation energy functional. ρ^{e} is the total electron charge density. $V_{i\ell}^{\mathrm{NL}}(\mathbf{r})$ is the nonlocal pseudopotential component on angular momentum ℓ for the atom i at position $\mathbf{R}_i$, and $\hat{P}_\ell$ is the projection operator for ℓ. V_{H} is the Hartree potential and V_i^{L} is the local part of the atomic pseudopotential centered at $\mathbf{R}_i$. Note we have chosen the positive-defined symmetric forms for the kinetic (t_0) and classic Coulomb (e_{CC}) energy densities[15]. The DFT total energy U^{DFT} and the energy density $\varepsilon(\mathbf{r})$ satisfy[16]:

$$
\begin{aligned}
U^{\mathrm{DFT}} =& \int\varepsilon(\mathbf{r})d\mathbf{r} - \frac{1}{2}\int d\mathbf{r}\sum_i \rho_i(\mathbf{r})V_i^{\mathrm{L}}(\mathbf{r}) \\
&+ \sum_{i\neq j}\frac{1}{2}\underbrace{[\frac{Z_iZ_j}{|\mathbf{R}_i - \mathbf{R}_j|} - \int d\mathbf{r}\rho_i(\mathbf{r})V_j^{\mathrm{L}}(\mathbf{r})]}_{V^{\mathrm{P}}(|\mathbf{R}_{ij}|)},
\end{aligned}
\qquad (5)
$$

where ρ_i is a fixed "smeared ion" charge density of atom i, defined as $\rho_i(\mathbf{r}) = -(1/4\pi)\nabla^2 V_i^{\mathrm{L}}(\mathbf{r})$, and Z_i and Z_j are the atomic valence charge of atom i and j. The integral of ρ_i equals to Z_i. The second term in Eq. 5 can be expressed as the sum of $E_{\mathrm{self}}(i) = (1/2)\int \rho_i(\mathbf{r})V_i^{\mathrm{L}}(\mathbf{r})d\mathbf{r}$, which is a constant for a given atom i. It thus doesn't contribute the heat current. The third term in Eq. 5 can be defined as a sum of pair interaction potentials $\sum_{i\neq j} V^{\mathrm{P}}(|\mathbf{R}_{ij}|)$. Hence, we have:

$$U^{\mathrm{DFT}} = \int\varepsilon(\mathbf{r})d\mathbf{r} - \sum_i E_{\mathrm{self}}(i) + \sum_{i\neq j} V^{\mathrm{P}}(|\mathbf{R}_{ij}|). \quad (6)$$

The pair term $V^{\mathrm{P}}(|\mathbf{R}_{ij}|)$ was not considered in Ref.[15]. Note, $\rho_i(\mathbf{r})$ is 0 beyond the cutoff radius r_c of the pseudopotential. As a result, $V^{\mathrm{P}}(|\mathbf{R}_{ij}|) = 0$ only when $|\mathbf{R}_{ij}| > 2r_c$. There are many cases where the nearest atom distance is smaller than $2r_c$, thus this term should not be dropped. Furthermore, in the plane wave implementation, due to the finite energy cut-off E_c of the

plane-waves used to represent ρ_i and V_j^{L}, $V^{\mathrm{P}}(|\mathbf{R}_{ij}|)$ can be long-ranged. To overcome such practical difficulty, we modified the ρ_i (thus the V_i^{L}) in reciprocal space for wave vector $|\mathbf{q}|$ larger than $q_c = \sqrt{2E_c}$. This modification ensure the finite range of $V^{\mathrm{P}}(|\mathbf{R}_{ij}|)$. The details are described in Ref.[16].

Besides the nonlocal term e^{NL}, all the other terms in $\varepsilon(\mathbf{r})$ involve only smooth local energy densities. They can be distributed into each atom using a partition function, following our procedure in Ref.[25], namely:

$$U_i^{\mathrm{DFT}} = \int d\mathbf{r}[t_0(\mathbf{r}) + e_{\mathrm{xc}}(\mathbf{r}) + e_{\mathrm{CC}}(\mathbf{r})]\frac{w_i(|\mathbf{r} - \mathbf{R}_i|)}{\sum_j w_j(|\mathbf{r} - \mathbf{R}_j|)}. \tag{7}$$

Here $w_i(|\mathbf{r}-\mathbf{R}_i|)$ is the isolated atom charge density. The total energy U^{DFT} can be written as:

$$U^{\mathrm{DFT}} = \sum_i[U_i^{\mathrm{DFT}} + E_i^{\mathrm{NL}} - E_{\mathrm{self}}] + \sum_{i\neq j} V^{\mathrm{P}}(|\mathbf{R}_{ij}|) \quad (8)$$

The choice of w_i, thus the energy partition, is not unique. However, provided w_i is local, different partitions will only redistribute the energy among the local nearest atoms. Since the thermal conductivity deals with macroscopic heat flow at a much larger scale, it should not be affected by such local energy redistribution. This is analogous to the assignment of atomic energy E_i in a pair potential FF $U(\mathbf{R}_{ij})$. $U(\mathbf{R}_{ij})$ does not need to be equally assigned to the two end atoms, especially if the two atom-types differs. This is also true for many-body potentials. Nevertheless, the G-K formula predicted thermal conductivity are insensitive to the definition of local energy, as long as the microscopic locality of the energy is maintained (i.e., no long-range energy re-assignment), as shown in Ref.[4,12]. The energy density $\varepsilon(\mathbf{r})$ itself of Eq. 4 is also not unique. But Ref.[9] showed such nonuniqueness will not affect the final thermal conductivity either. Finally, the atomic energy E_i in Eq. 2 can be written as:

$$E_i = \frac{1}{2}m_i\mathbf{v}_i^2 + U_i^{\mathrm{DFT}} + E_i^{\mathrm{NL}} - E_{\mathrm{self}} + \sum_j V^{\mathrm{P}}(|\mathbf{R}_{ij}|), \quad (9)$$

where m_i is the atom mass.

After E_i is obtained at every MD step, another challenge is the ill-definition of $\mathbf{R}_i$ in the second term of Eq. 2 in a periodic system. The same problem exists in the calculation of polarization[26]. Here we introduce a two-step approach to solve this problem. Note if we can find a boundary for an isolate region, where there is no heat (energy) flow crossing this boundary, then the $\mathbf{r}$ issue will disappear, since $\mathbf{r}$ can be defined inside this region without the periodic wrapping problem (note an arbitrary constant on $\mathbf{r}$ exists due to the definition of origin. But it will have zero effect since $\sum_i dE_i/dt = 0$ within this isolated region). However, usually there is no such zero-heat-current boundary (ZHCB) for a given MD step. Here, we will create such a ZHCB by moving the atoms in two steps retrospectively after each normal MD step

movement. More specifically, consider that the movement of atom i between the two MD steps N and $N+1$ is $\triangle\mathbf{R}_i$. Assuming x is the direction of interest, we introduce a 1D mask function $m(x)$ defined in [0,1] with the shape shown in Fig. 1a. $m(x)=0$ when x is close to 0 or 1, whereas $m(x)=1$ for x around 0.5. In the present work we use $m(x) = [\mathrm{erfc}(12|x-0.5|-3)]/2$. Then we create an intermediate step $N+0.5$, and divide the movement $\triangle\mathbf{R}_i$ into two sub-steps. In the first sub-step (N to $N+0.5$), the atomic movement is $\triangle\mathbf{R}'_i = m(x_i/L_\mathrm{x})\triangle\mathbf{R}_i$, and in the second sub-step ($N+0.5$ to $N+1$), the atomic movement is $\triangle\mathbf{R}''_i = [1 - m(x_i/L_\mathrm{x})]\triangle\mathbf{R}_i$. Here $x_i \in [0, L_\mathrm{x})$ is the x coordination of atom i before the movement, and L_x is the supercell length along x. A DFT self-consistent calculation is done for $N+0.5$ to get the U_i^{DFT} in this step. In the first sub-step, the atoms whose x_i is close to 0 or L_x are fixed. Since the energy density is a local property, U_i^{DFT} only depends on the local environment, thus dU_i^{DFT}/dt for these atoms will be zero if the supercell is sufficiently long along x. The kinetic energy change equals to $\mathbf{F}_i \cdot \triangle\mathbf{R}'_i$ ($\mathbf{F}_i$ is the atomic force), which is also zero at $x_i=0$. This will give a ZHCB at $x=0$ (or L_x). Similarly, in the second sub-step, there will be a ZHCB at $x=L_\mathrm{x}/2$. Within each substep, the heat current along x can be properly calculated by choosing $\mathbf{R}_i$ from the center of the movement zone, as shown in Fig. 1b. Putting the two substeps together we have:

$$J_\mathrm{x} = \sum_i E_i v_i^\mathrm{x} + \sum_i (\widetilde{x}_i^\mathrm{I} \frac{dE_i^\mathrm{I}}{dt} + \widetilde{x}_i^\mathrm{II} \frac{dE_i^\mathrm{II}}{dt}). \qquad (10)$$

Here v_i^x is the x component of velocity. $\widetilde{x}_i^\mathrm{I}$ and $\widetilde{x}_i^\mathrm{II}$ are the x components of $\mathbf{R}_i$ for the atom movement domain in substep I and II, respectively, with their origins defined at the center of the corresponding domains. dE_i^I and dE_i^II are the change in E_i in substep I and II. Using this J_x, the thermal conductivity along x can then be calculated according to Eq. 1. The computational cost of this approach is only twice (due to the two-step process) as that of an ordinary FP-MD. Our test calculations on crystal Lennard-Jones argon[16] show that this two-step method (Eq. 10) is equivalent to the commonly used pair-force method (Eq. 3). This technique can also be used for the dipole moment change in a periodic system due to atomic displacements, which is often calculated using Berry phase method[27].

With E_i and the two-step approach, we can now apply the Green-Kubo method to first-principles molecular dynamic (FP-MD) simulations. The FP-GK method is implemented in PWmat[28], a GPU based plane-wave pseudopotential code for DFT simulations. The norm-conserving pseudopotentials[29] and the LDA functional[30] are used. Detailed simulation setups for all test systems are given in Ref.[16]. We also did parameter tests on the form of $m(x)$, on the LDA atomic-energy dependence radius, and on the number of trajectories used.[16] The tests showed our setup was appropriate. To test the feasibility of the FP-GK method, following Ref.[9], we first choose the
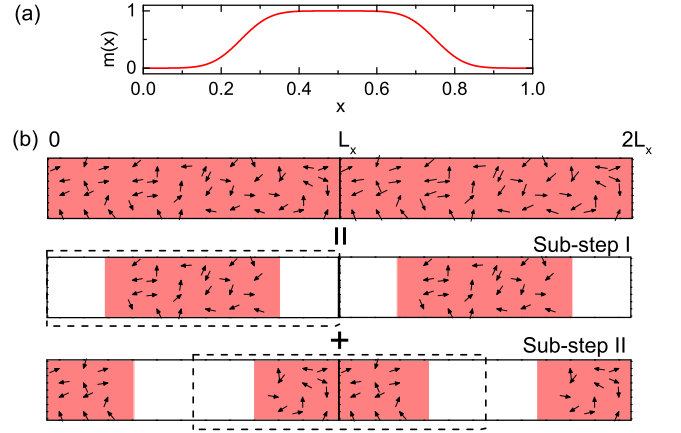

FIG. 1. (a) The mask function $m(x)$. (b) Illustration of the two sub-steps. The solid lines indicate the supercell, and L_x is the cell length along x. The arrows denote the atomic movement in a MD step. It is divided into two sub-steps according to the mask function. Regions with zero and non-zero heat current are marked by white and red, respectively. The heat current can be properly calculated if the supercell boundaries lie inside the zero-heat-current regions, as indicated by the dash lines.
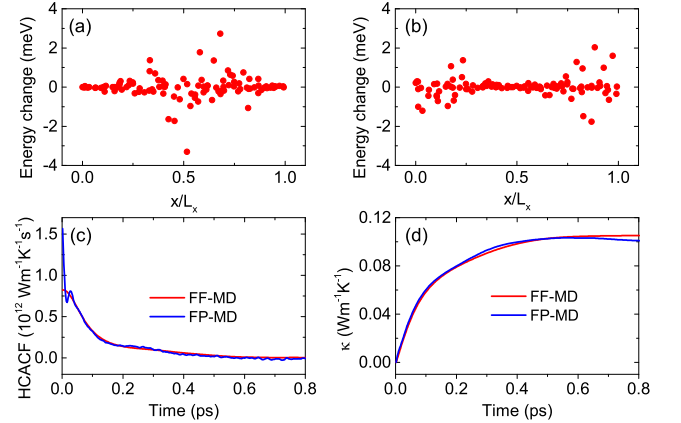

FIG. 2. (a)-(b) Typical change of atomic energy E_i in the first (a) and second (b) sub-steps for LDA-Ar. Each point stands for one atom. x/L_x is the fraction x coordination of atoms. (c) The HC-ACF (multipled by the factor $1/k_\mathrm{B}T^2 V$) and (d) the thermal conductivity κ of LDA-Ar at 400 K.

liquid argon with LDA exchange-correlation functional (LDA-Ar) as a demonstration system. The interaction between LDA-Ar atoms can be fitted by a classic pair potential, thus allows one to directly compare the results between FP-MD and FF-MD. In this inert element case, we expect the pair potential result to be good. We fit the DFT calculated energy of two Ar atoms of a distance r with the pair potential (See Ref.[16] for fitting details): $U(r) = (a_1 r^2 + a_2 r + a_3)e^{-a_4 r} + E_0$, and use this potential for the reference FF-MD simulation, same as in Ref.[9]. The thermal conductivity of liquid LDA-Ar is calculated by both FP-MD and FF-MD.

We first look at the DFT calculated atomic energies E_i. Figs. 2a and 2b show the typical changes of E_i in the first and second MD sub-steps. For the first sub-step, the energies of the atoms near the cell center ($x_i = 0.5L_x$) changes significantly, whereas the atoms near the cell boundary ($x_i = 0$ and $x_i = L_x$) have negligible energy change, and vice versa for the second sub-step. Similar trends were observed throughout the whole FP-MD trajectories. Therefore, ZHCB are clearly generated in this not-so-large supercell (108 atoms). These results indicate that the DFT atomic energy E_i depends only on the local atomic environment. This is an important feature making our final result independent of the details of the local energy partition.

Fig. 2c and 2d show the HC-ACF and the thermal conductivity κ calculated from FP-MD and FF-MD for liquid Ar at 400K. Both methods give very similar results. The HC-ACF decays to 0 after $\sim$0.6 ps, and both methods obtain a κ of 0.1 Wm^{-1}K^{-1}. This also agrees with Ref.[9] where both G-K and non-equilibrium DFT calculations found the κ at around 0.1 Wm^{-1}K^{-1} for the same system. This result shows our FP-GK method works by reproducing the FF G-K result, as well as previous first-principles results, and it is rather practical to carry out the FP-GK calculations for systems with small κ (hence relatively short decay time in the HC-ACF).

Just as Ref.[9], the LDA-Ar system is only for proof-of-concept purpose as LDA cannot capture the van der Waals interactions. Next we apply the FP-GK method to amorphous silicon, where the covalent bonds between the Si atoms provide strong non-trivial many-body interactions. Such system is also difficult to be studied using the anharmonic interaction approach since the number of possible three-body anharmonic terms is huge due to the lack of translational symmetry[2]. On the other hand, the phonon scattering is strong, thus the HC-ACF decays fast, and short simulation times should be sufficient (provided many trajectories are simulated). The FP-GK calculated HC-ACF and κ for amorphous Si at 300 K is presented in Fig. 3a and 3b. Due to limited simulation time and ensembles, the HC-ACF doesn't decay to 0 monotonously, but with some oscillations. Despite the oscillations, κ is essentially not increasing beyond 3 ps. Therefore, we take the average value of κ in the region of 3-4 ps to estimate the converged value, which is determined to be 1.4 Wm^{-1}K^{-1}. This is two orders of magnitude smaller than that of crystal Si[31]. The predicted κ is consist with various reported experimental[32–34] and theoretical[35–37] values in the range of 1-2 Wm^{-1}K^{-1}. Note that in principle there is no qualitative difference between amorphous Si and crystal Si, except for the much longer phonon scattering time in the latter. The validity of the FP-GK method on amorphous Si suggests that one can also apply it to crystal Si, provided that sufficiently long MD trajectories (at ns scale) will be used (see Ref.[16]).

As a third example, we calculate the thermal conductivity of liquid Si at 2000 K using the FP-GK method,
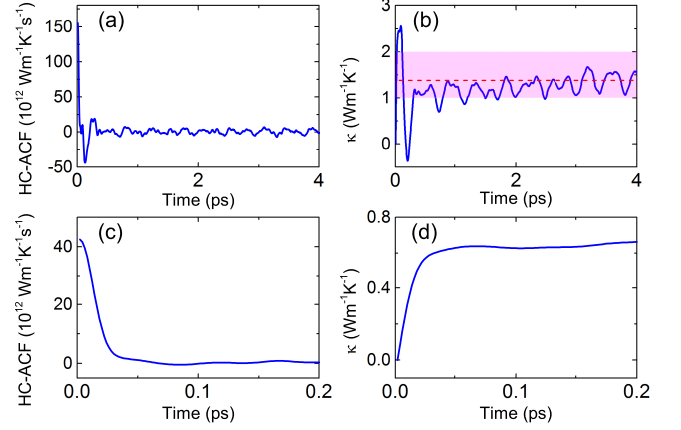

FIG. 3. The HC-ACF (multipled by the factor $1/k_B T^2 V$) and lattice thermal conductivity κ for amorphous Si at 300 K (a)-(b) and liquid Si at 2000 K (c)-(d). The dashed lines in (b) indicates the average value of κ in [3,4] ps. The pink region indicates the range of κ reported in previous studies[32–37].

and the results are presented in Figs. 3c and 3d. Liquid Si is a metal, and its thermal conductivity is dominated by electron[38], while the contribution from lattice phonon is quite small. The phonon relaxation in liquid Si is fast, as the HC-ACF decays to 0 within 100 fs (Fig. 3c). The κ is found to be 0.63 Wm^{-1}K^{-1}, only 1% of the experiment measured total thermal conductivity ($\sim$ 60 Wm^{-1}K^{-1})[38,39]. Baker et al. predicted a lattice thermal conductivity of 1.78 Wm^{-1}K^{-1} for the same system using the Stillinger-Weber potential.[40] The result qualitatively agrees with ours, and the quantitative difference could come from the difference between the Stillinger-Weber potential and LDA. Although the Stillinger-Weber potential is good for ground state Si structure, it overestimates the lattice thermal conductivity of Si crystal by 40% when the temperature is close to the melting point[40].

In summary, we presented a new FP-GK approach to calculate the thermal conductivity of materials. Compared to the approach in Ref.[9], it does not need the calculation of linear equations at each MD step. The computational cost is only twice as that of an ordinary FP-MD. Compared to the method of Ref.[11], it does not drop the convection current and can be used for liquid simulations, as well as pseudopotential calculations. In this method we use a partition scheme to assign the DFT energy into each atom. Moreover, we introduce a two-step approach to solve the problem of periodic system wrapping effect for the position $\mathbf{R}_i$. The FP-GK method is particularly practical for disorder systems (e.g., solid amorphous or liquid) at high temperature where the phonon scattering is strong and the thermal conductivity is small. Thus the HC-ACF decay fast and short picosecond FP-MD simulations will be sufficient. The calculated Ar-liquid, Si-amorphous and Si-liquid thermal conductivities agree well with previous theoretical results and experimental

measurements.

ACKNOWLEDGMENTS

[*] lwwang@lbl.gov

[1] D. A. Broido, M. Malorny, G. Birner, N. Mingo, and D. A. Stewart, Appl. Phys. Lett. **91**, 231922 (2007).

[2] F. Zhou, W. Nielson, Y. Xia, and V. Ozoliņš, Phys. Rev. Lett. **113**, 185501 (2014).

[3] A. Tenenbaum, G. Ciccotti, and R. Gallico, Phys. Rev. A **25**, 2778 (1982).

[4] P. K. Schelling, S. R. Phillpot, and P. Keblinski, Phys. Rev. B **65**, 144306 (2002).

[5] M. S. Green, J. Chem. Phys. **22**, 398 (1954).

[6] R. Kubo, M. Yokota, and S. Nakajima, J. Phys. Soc. Jpn **12**, 1203 (1957).

[7] D. McQuarrie, *Electronic Transport in Mesoscopic Systems* (University Science Books, Sausalito, 2000).

[8] A. J. McGaughey and J. M. Larkin, Ann. Rev. Heat Trans. **17**, 49 (2014).

[9] A. Marcolongo, P. Umari, and S. Baroni, Nat. Phys. **12**, 80 (2015).

[10] S. Baroni, S. de Gironcoli, A. Dal Corso, and P. Giannozzi, Rev. Mod. Phys. **73**, 515 (2001).

[11] C. Carbogno, R. Ramprasad, and M. Scheffler, Phys. Rev. Lett. **118**, 175901 (2017).

[12] P. C. Howell, J. Chem. Phys. **137**, 224111 (2012).

[13] Z. Fan, L. F. C. Pereira, H.-Q. Wang, J.-C. Zheng, D. Donadio, and A. Harju, Phys. Rev. B **92**, 094301 (2015).

[14] A. McGaughey and M. Kaviany, Int. J. Heat Mass Transfer, **47**, 1783 (2004).

[15] M. Yu, D. R. Trinkle, and R. M. Martin, Phys. Rev. B **83**, 115113 (2011).

[16] See Supplemental Material for the integral of energy density, optimization of smeared ion charge density, thermal conductivity of L-J argon using the two step method, pair potential fitting for LDA-Argon, setup of thermal conductivity calculations, parameter tests, and disucssions on crystal Si calculation. Refs. [2],[9],[11],[17-24] are included in the supplemental material.

[17] L.-W. Wang, Phys. Rev. B **64**, 201107 (2001).

[18] K. V. Tretiakov and S. Scandolo, J. Chem. Phys. **120**, 3765 (2004).

[19] S. Plimpton, J. Comput. Phys. **117**, 1 (1995).

[20] A. C. T. van Duin, S. Dasgupta, F. Lorant, and W. A. Goddard, J. Phys. Chem. A **105**, 9396 (2001).

[21] S. Kugler, L. Pusztai, L. Rosta, P. Chieux, and R. Bellissent, Phys. Rev. B **48**, 7685 (1993).

[22] R. Vogelsang, C. Hoheisel, and G. Ciccotti, J. Chem. Phys. **86**, 6371 (1987).

[23] K. Gordiz, D. J. Singh, and A. Henry, J. Appl. Phys. **117**, 045104 (2015).

[24] L.-W. Wang, Phys. Rev. B **72**, 045417 (2005).

[25] L.-W. Wang, Phys. Rev. Lett. **88**, 256402 (2002).

[26] R. Resta and D. Vanderbilt, "Theory of polarization: A modern approach," in *Physics of Ferroelectrics: A Modern Perspective* (Springer Berlin Heidelberg, Berlin, Heidelberg, 2007).

[27] R. D. King-Smith and D. Vanderbilt, Phys. Rev. B **47**, 1651 (1993).

[28] http://www.pwmat.com/.

[29] M. Fuchs and M. Scheffler, Comput. Phys. Commun. **119**, 67 (1999).

[30] D. M. Ceperley and B. J. Alder, Phys. Rev. Lett. **45**, 566 (1980).

[31] C. J. Glassbrenner and G. A. Slack, Phys. Rev. **134**, A1058 (1964).

[32] B. L. Zink, R. Pietri, and F. Hellman, Phys. Rev. Lett. **96**, 055902 (2006).

[33] D. G. Cahill, H. E. Fischer, T. Klitsner, E. T. Swartz, and R. O. Pohl, J. Vac. Sci. Technol. A **7**, 1259 (1989).

[34] H. Wada and T. Kamijoh, Jpn. J. Appl. Phys. **35**, L648 (1996).

[35] J. M. Larkin and A. J. H. McGaughey, Phys. Rev. B **89**, 144303 (2014).

[36] Y. H. Lee, R. Biswas, C. M. Soukoulis, C. Z. Wang, C. T. Chan, and K. M. Ho, Phys. Rev. B **43**, 6573 (1991).

[37] P. B. Allen and J. L. Feldman, Phys. Rev. Lett. **62**, 645 (1989).

[38] H. Kobatake, H. Fukuyama, I. Minato, T. Tsukada, and S. Awaji, Appl. Phys. Lett. **90**, 094102 (2007).

[39] E. Yamasue, M. Susa, H. Fukuyama, and K. Nagata, J. Cryst. Growth **234**, 121 (2002).

[40] C. H. Baker, C. Wu, R. N. Salaway, L. V. Zhigilei, and P. M. Norris, Int. J. Trans. Phenomena **13**, 143 (2012).